BEILSTEIN ARCHIVES

This open access document is posted as a preprint in the Beilstein Archives at https://doi.org/10.3762/bxiv.2026.4.v1 and is considered to be an early communication for feedback before peer review. Before citing this document, please check if a final, peer-reviewed version has been published.

This document is not formatted, has not undergone copyediting or typesetting, and may contain errors, unsubstantiated scientific claims or preliminary data.

Preprint Title	Sustainable fabrication of 2D-based devices through reuse of substrates with microfabricated electrodes
Authors	Ying Zhang, Yigit Sozen, Esteban Zamora-Amo, Thomas Pucher, Nuria Jiménez-Arévalo, Zdenek Sofer, Yong Xie and Andres Castellanos-Gomez
Publication Date	28 Jan. 2026
Article Type	Full Research Paper
Supporting Information File 1	Supporting_Information.docx; 10.4 MB
ORCID® iDs	Ying Zhang - https://orcid.org/0009-0008-8358-1045; Thomas Pucher - https://orcid.org/0009-0005-2100-8241; Yong Xie - https://orcid.org/0000-0001-7904-664X; Andres Castellanos-Gomez - https://orcid.org/0000-0002-3384-3405

License and Terms: This document is copyright 2026 the Author(s); licensee Beilstein-Institut.

This is an open access work under the terms of the Creative Commons Attribution License (https://creativecommons.org/licenses/by/4.0). Please note that the reuse, redistribution and reproduction in particular requires that the author(s) and source are credited and that individual graphics may be subject to special legal provisions. The license is subject to the Beilstein Archives terms and conditions: https://www.beilstein-archives.org/xiv/terms.
The definitive version of this work can be found at https://doi.org/10.3762/bxiv.2026.4.v1

Sustainable fabrication of 2D-based devices through reuse of substrates with microfabricated electrodes

Ying Zhang[1,2], Yigit Sozen[1,2], Esteban Zamora-Amo[1,2], Thomas Pucher[1,2], Nuria Jiménez-Arévalo[1], Zdenek Sofer[3], Yong Xie*[1, 4], Andres Castellanos-Gomez*[1]

Address: [1]2D Foundry research group. Instituto de Ciencia de Materiales de Madrid (ICMM-CSIC), Madrid, 28049, Spain and [2]Universidad Autónoma de Madrid, Escuela de Doctorado, Madrid, 28049, Spain and [3]Department of Inorganic Chemistry, University of Chemistry and Technology, Prague, Prague, Czech Republic and [4]School of Advanced Materials and Nanotechnology, Xidian University, 710071 Xi'an, China

Email: Yong Xie - yxie@xidian.edu.cn; Andres Castellanos-Gomez - andres.castellanos@csic.es

Abstract

Fabricating microelectronic devices for two-dimensional (2D) materials research is essential but often limited by the high cost and need for specialized facilities. This study presents an efficient and sustainable method for cleaning and reusing substrates with pre-patterned electrodes. The cleaning protocol involves the use of an ultrasonic bath in warm N-methyl-2-pyrrolidone (NMP), enabling the removal of 2D materials without damaging the electrodes. This method significantly reduces costs and encourages more responsible use of resources in 2D materials device fabrication.

Keywords

2D device fabrication; microfabricated electrode; N-methyl-2-pyrrolidone; substrate reuse; ultrasonic cleaning

Introduction

Nanoscience research often needs the fabrication of proof-of-concept devices to demonstrate applications of novel nanomaterials or to study their fundamental properties.[1–4] Creating these microelectronic devices requires access to highly specialized infrastructure like cleanrooms and trained personnel.[5–7] Consequently, research groups focused on nanomaterials synthesis may lack the resources to integrate their novel nanomaterials into microelectronic devices, potentially reducing the impact of their research.

To address this issue, commercially available substrates with pre-patterned electrodes, ready to integrate the nanomaterial under study present an optimal solution.[7–9] In recent years, our team has regularly employed this strategy, transferring two-dimensional (2D) materials onto pre-patterned electrodes to create devices such as transistors, photodetectors, and diodes.[10–15] However, this approach incurs significant costs, approximately 40-50 € per chip for custom-made electrodes. Therefore, developing a method to clean and reuse these devices is highly desirable.

Several recent studies have explored substrate reuse strategies to mitigate fabrication costs and improve sustainability in device prototyping.[16–18] For example, Bhalla et al. investigated various cleaning and regeneration techniques for electrochemical sensor chips, comparing piranha, plasma, oxidative, and reductive electrochemical cleaning methods.[19] Similarly, Stan et al. showed different cleaning methods for screen-printed gold electrodes and identified optimal techniques that allow their reuse

in electrochemical applications, preserving electrode performance.[20] Furthermore, Fakhr et al. explored cleaning methods for gold electrodes on diverse substrates and found that chemical treatments such as KOH and H_2O_2 effectively restore the substrate surface, allowing their application in reusable biosensors.[21] A different approach to reuse the substrates was reported by Paupy et al. by developing wafer-scale detachable monocrystalline germanium nanomembranes for III-V material growth and substrate reuse, significantly reducing material waste and enabling repeated use of substrates in epitaxial growth applications.[22]

Inspired by these approaches, we propose a robust and reproducible cleaning process for reusing microfabricated substrates with pre-patterned electrodes in 2D materials research. Unlike prior studies that primarily focus on epitaxial growth or electrochemical sensing applications, our method is specifically designed to facilitate the reuse of substrates for 2D material-based electronic devices. Our approach involves deep cleaning in an ultrasonic bath with N-methyl-2-pyrrolidone (NMP) at 50 °C,[23,24] followed by an acetone and isopropyl alcohol (IPA) rinse, and nitrogen blow-drying to ensure complete removal of residual 2D materials and adhesives. This method ensures that the pre-patterned electrodes remain intact while achieving effective surface cleaning for subsequent nanomaterial deposition.

By implementing this cleaning protocol, we demonstrate that substrates can be reliably reused without compromising device performance, ultimately reducing fabrication costs and making microelectronic prototyping more accessible to research groups without cleanroom facilities. This study contributes to the growing body of work on sustainable use of resources in research environments and provides a practical solution for extending the usability of expensive microelectronic substrates.

Results and Discussion

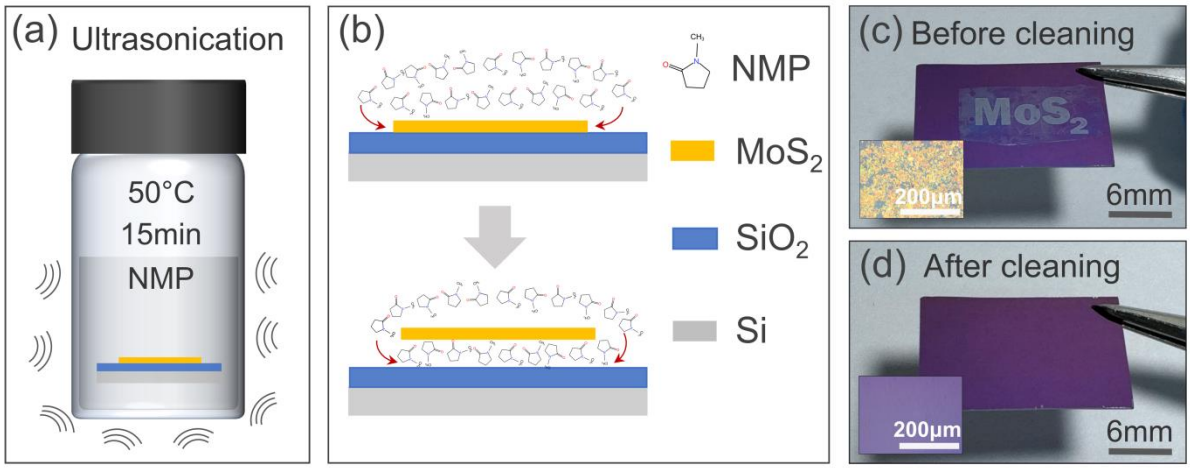

Figure 1: Demonstration of the ultrasonic cleaning process for substrate reuse. (a) Schematic diagram illustrating the ultrasonic cleaning setup with N-methyl-2-pyrrolidone (NMP) at 50 °C to remove MoS_2 flakes and adhesive residues from the substrate. (b) Schematic representation illustrates the removal of MoS_2 flakes from the substrate through the penetration of N-methyl-2-pyrrolidone (NMP) at at 50 °C. (c) Optical images of the substrate before and after the removal of MoS_2 flakes fabricated via roll-to-roll mechanical exfoliation.

Figure 1a presents a schematic illustration of the cleaning process: the chip with pre-patterned electrodes that needs to be cleaned is immersed in NMP and placed in an ultrasonic bath at 50 °C. The effectiveness of the ultrasonic cleaning process in hot NMP arises from the interaction between NMP molecules and the interface between the 2D material flakes and the SiO_2/Si substrate. NMP is known for its strong affinity for surface contaminants and its ability to penetrate microscopic gaps.[24] When heated to 50 °C, the solvent reduces adhesion forces by weakening van der Waals interactions between the 2D flakes and the substrate. Simultaneously, ultrasound agitation enhances molecular diffusion and promotes cavitation, generating localized

pressure fluctuations that further assist in lifting the flakes. As a result, NMP molecules wedge between the 2D material and the SiO_2 surface, effectively detaching the flakes and enabling their complete removal without damaging the underlying electrodes (see schematic illustration in Figure 1(b)).

To evaluate the effectiveness of the cleaning protocol, we applied it to a SiO_2/Si substrate covered with a film composed of a network of MoS_2 flakes prepared by high-throughput roll-to-roll mechanical exfoliation (transfer 5 times to obtain the continuous film).[25,26] This method enables a high surface coverage of densely packed flakes that adhere strongly to the substrate, making it a more challenging and representative benchmark for cleaning compared to conventional manual exfoliation, which typically results in sparsely distributed flakes that are easier to remove. The MoS_2 film was patterned using a vinyl stencil mask, producing a well-defined 'MoS_2' pattern on the substrate surface. As shown in Figure 1c, prior to cleaning, the substrate exhibited both the patterned MoS_2 network and residual adhesive from the stencil mask around the 'MoS_2' area. Following the ultrasonic bath in hot NMP and subsequent rinsing in isopropanol, all MoS_2 flakes and adhesive residues were completely removed, leaving a pristine SiO_2/Si surface (Figure 1d). The insets in Figure 1(c) and (d) provide high-magnification optical microscopy images. Before cleaning, the interconnected network of MoS_2 flakes is visible, whereas after treatment, the surface appears clean and free of contaminants. The rationale for selecting NMP as the cleaning solvent and 50 °C as the operating temperature is discussed in detail in the Supporting Information (see Figures S1-S3) by comparing with other solvents and process temperatures.

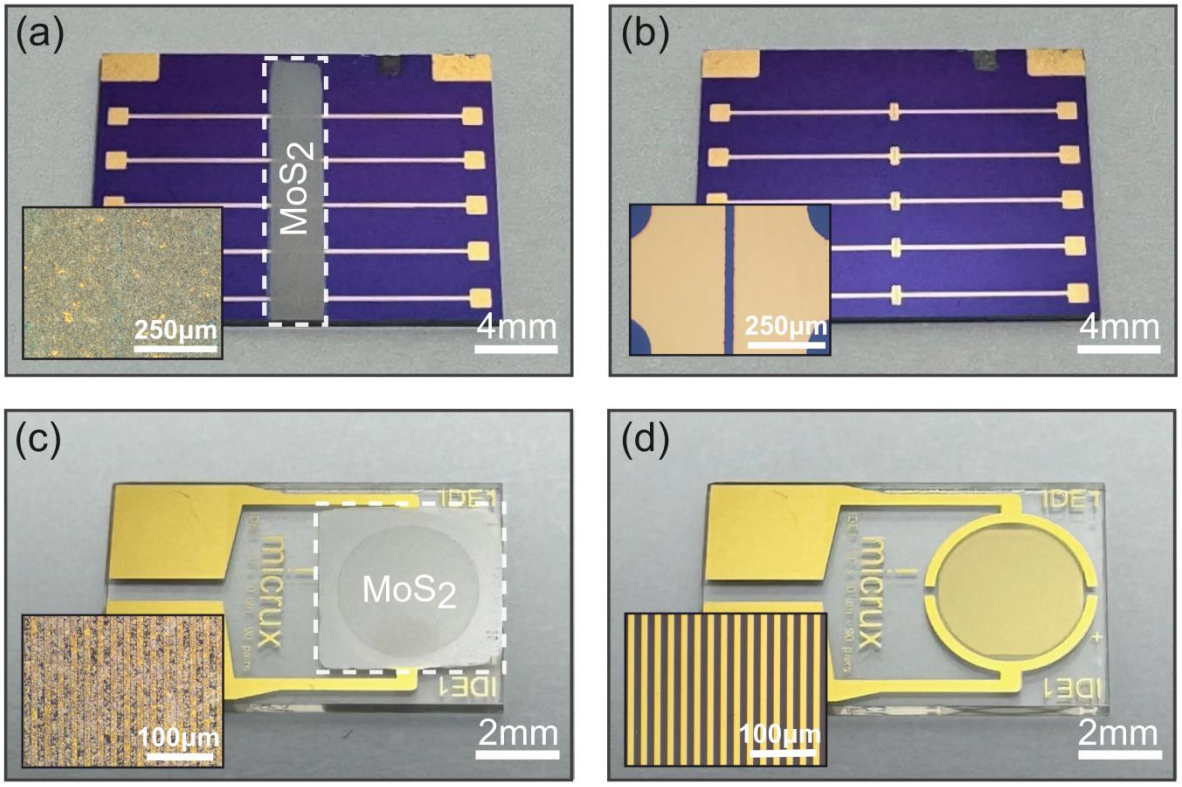

Figure 2: Substrates with different pre-patterned electrodes before and after cleaning. (a-b) Macroscopic images of a SiO_2/Si substrate with five printed drain-source gold electrodes (channel length: 25 µm). A large amount of MoS_2 flakes were transferred onto the electrode regions prior to cleaning procedure, as shown in (a). Images were taken before (a) and after (b) the cleaning process. Insets show representative optical microscopy images for each case. (c-d) Macroscopic images of a interdigitated electrode (by Micrux) with the channel length of 10 µm. MoS_2 films had been transferred onto the electrode regions prior to cleaning, as shown in (c). Images were taken before (c) and after (d) the cleaning process. Insets show representative optical microscopy images for each case. Dashed box outlines the MoS_2 film region.

To demonstrate that this method is broadly applicable, Figure 2 presents different pre-patterned electrode configurations before and after undergoing the proposed cleaning

process. Figure 2(a) and (b) show drain-source electrode structures pre-patterned on a SiO_2/Si substrate, commonly used in field-effect transistor (FET) fabrication, initially covered with a large-scale MoS_2 film produced by roll-to-roll mechanical exfoliation. Figure 2(c) and (d) display interdigitated electrodes with a 10 µm gap separation, fabricated on glass, widely used for electrochemisty and biosensing applications.[27] For both cases, the cleaning process effectively removes the MoS_2 flakes while preserving the structural integrity of the electrodes. The insets in Figure 2 provide zoomed-in optical images that further illustrate the removal of material from the electrode gaps. In addition to the cleaning of films of roll-to-roll mechanically exfoliated van der Waals materials, we investigated the cleaning and reuse of substrates with chemical vapour deposition (CVD)-grown MoS_2 flakes (see Supporting Information Figure S4).[28,29]

To rigorously evaluate whether the cleaning method enables real and practical reuse of the substrates, we performed multiple cycles of device fabrication, electrical characterization, and subsequent cleaning on a pre-patterned SiO_2/Si chip (similar to the one shown in Figure 2a and 2b). MoS_2 flakes obtained via roll-to-roll mechanical exfoliation were sequentially transferred onto the same pre-patterned electrodes to fabricate three FETs.[25,30] After each fabrication, the drain-source current versus bias voltage (I-V) characteristics were measured at different gate voltages, as shown in Figure 3(a-c). Following the electrical characterization, the samples underwent the cleaning process, and the substrates were tested to verify the absence of any electrical connections between the electrodes. The insets in Figures 3(a-c) show the electrical characterization after each cleaning process, confirming the lack of residual conductivity, indicating the complete removal of MoS_2 flakes and any potential contaminants.

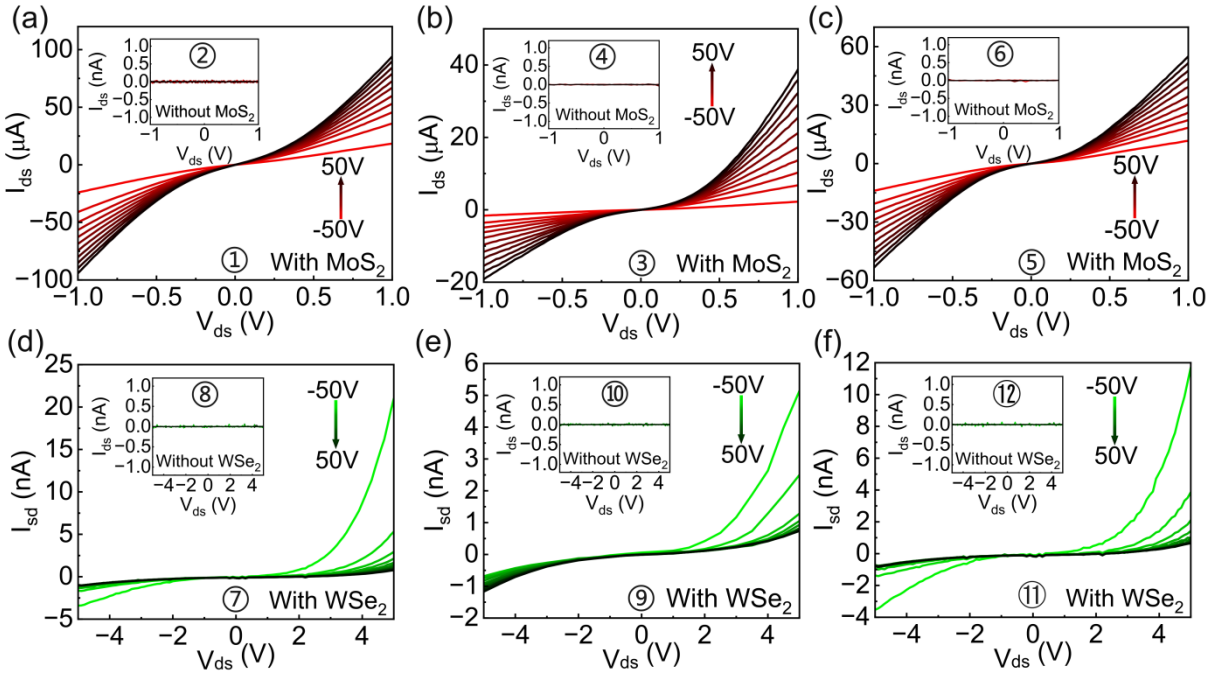

Figure 3: Repeated characterization of MoS_2- and WSe_2-based FETs on the same pre-patterned SiO_2/Si chip before and after multiple cleaning processes. (a-c) Drain-source current versus bias voltage characteristics of the devices at different gate voltages of the first, second and third MoS_2-based FETs. (d-f) Drain-source current versus bias voltage characteristics of the devices at different gate voltages of the first, second and third WSe_2-based FETs, following three successful MoS_2-based FETs. The insets in each plot present the drain-source current versus bias voltage characteristics of the same sample measured after each successive cleaning step.

Although some variations were observed in the electrical characteristics of the re-fabricated FETs, this is expected due to the inherent stochastic nature of the MoS_2 films fabricated by roll-to-roll mechanical exfoliation, which consist of a network of interconnected flakes.[25] Nonetheless, the consistency in device performance across multiple fabrication cycles demonstrates the reliability of the cleaning process in preserving the integrity of the pre-patterned electrodes and ensuring effective reuse of the substrates.

To assess the applicability of this cleaning method to other 2D materials, we extended the study to WSe_2-based devices. After three successful cycles with MoS_2, we transferred WSe_2 flakes onto the same cleaned electrodes and fabricated three additional FETs following the same procedure, as shown in Figure S5. The electrical characteristics of these devices were measured before and after each cleaning cycle (as shown in Figure 3(d-f)), confirming that the cleaning method effectively removes both MoS_2 and WSe_2 flakes without degrading the electrodes. These results validate the robustness of our method for the repeated fabrication of 2D material-based electronic devices and highlight its potential for enabling a sensible use of resources in microfabrication practices.

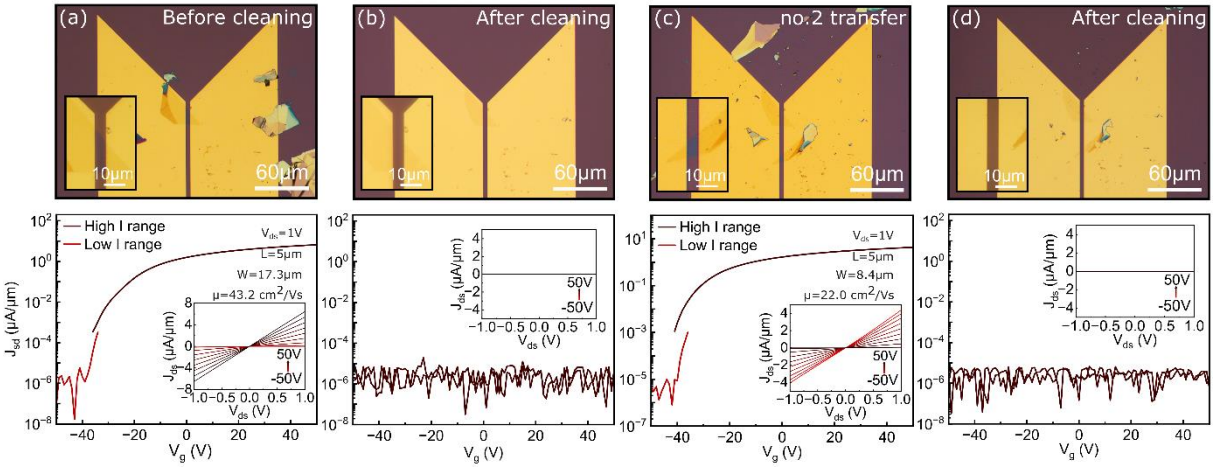

Figure 4: Reproducible fabrication, cleaning, and characterization of monolayer MoS_2 FETs on the same pre-patterned chip. (a, b) Microscopic images of the first monolayer MoS_2 flake bridging the source-drain electrodes before and after cleaning, together with the transfer characteristics and drain-source current versus bias voltage characteristics at different gate voltages. (c, d) Microscopic images and electrical characteristics of a second monolayer MoS_2 flake transferred onto the same electrodes before and after cleaning. Insets in each panel show magnified macroscopic images of the monolayer MoS_2 region before and after cleaning.

To further proof the general character of the cleaning method, we also tested the MoS_2 and WSe_2 films on indium tin oxide (ITO) substrate (shown in Supplementary Information Figure S6). The fabrication and cleaning procedures were carried out as previously described in this work. As shown in Figure S7, the electrical characterization of the devices before and after cleaning confirms the highly effective removal of MoS_2 and WSe_2 flakes, with no visible residues. Additionally, the ITO electrodes remained intact, as proved by the lack of electrical degradation after repeated use, indicating stable device fabrication and reliable substrate reusability.

Beyond the roll-to-roll deposited films of 2D materials, it is crucial to evaluate the reusability of substrates in the context of devices fabricated with single mechanically exfoliated flakes or chemical vapor deposition (CVD)-grown films (approaches more commonly adopted in the literature). To this end, we demonstrate the recycling of a pre-patterned electrode substrate for fabricating single-flake MoS_2 field-effect transistors (FETs). Single-layer MoS_2 flakes were identified using transmission-mode optical microscopy and confirmed via differential reflectance spectroscopy.[31–33] A selected flake was then transferred using an all-dry deterministic method to bridge a pair of gold electrodes (Figure 4a, top).[34] After high-vacuum annealing, the device was electrically characterized in a custom high-vacuum probe station.[35] Figure 4a (bottom) presents representative output and transfer characteristics of the single-layer MoS_2 FET, displaying an on/off current ratio of 3.4×10^6 and a field-effect mobility of 43.2 $cm^2/V\cdot s$.

Following characterization, the device underwent the deep cleaning protocol. The process effectively removed the MoS_2 from the channel region and detached most multilayer residues. However, small remnants of the monolayer in direct contact with the gold electrodes remained (see inset in Figure 4b), likely due to the strong chemical

affinity between MoS_2 and gold (a mechanism exploited in gold-assisted exfoliation methods).[36,37] Interestingly, in devices that had not been annealed, the entire flake was more easily removed, presumably due to weaker adhesion resulting from interfacial adsorbates or trapped air (see Supporting Information Figure S8).

Despite the incomplete removal of monolayer at the gold contacts, the electrodes remained electrically isolated after cleaning, as confirmed by the open-circuit behavior shown in Figure 4b. A new flake was then transferred a few microns away, forming a second FET that exhibited typical device performance (Figure 4c), the on/off current ratio is 8.5×10^5 and the field-effect mobility is 22.0 $cm^2/V{\cdot}s$. Finally, the device was subjected to an additional cleaning cycle, restoring the substrate for further reuse (Figure 4d), thus completing the full reusability cycle.

Conclusions

The ability to efficiently reuse microelectronic substrates with pre-patterned electrodes offers significant advantages, both in terms of cost savings and efficient use of lab resources. In this work we have developed and validated a highly effective cleaning method for the reuse of microelectronic substrates with pre-patterned electrodes. Using an ultrasonic bath in NMP, followed by IPA rinsing and nitrogen drying. The cleaning method presented in this study effectively removes nanomaterial residues, restoring the substrate to a near-original state, as demonstrated by the electrical characterization of devices. This approach could be applied to a wide variety of nanomaterials and electrode configurations, making it highly adaptable to different research needs.

By reducing the number of single-use substrates and minimizing waste, this method also contributes to more sustainable research practices. Future work could explore the

application of this cleaning protocol to other material systems and substrates, as well as further quantify the long-term durability of reused substrates across multiple cycles.

Experimental

Pre-patterned electrodes fabrication

Pre-patterned electrodes were fabricated by placing, the shadow masks (Ossila E291) onto the SiO_2(290nm)/Si(p++) substrates, followed by the deposition of 5nm Ti/45nm Au via the electron beam evaporation. The interdigitated electrodes on glass were supplied from Micrux Technologies and the interdigitated ITO electrodes on glass were purchased from Ossila (S161-20).

Materials preparation

The MoS_2-based samples were prepared using natural bulk molybdenite mineral (Molly Hill Mine, Quebec, Canada). WSe_2 crystals were prepared by CVT method from tungsten and selenium using bromine as a transport agent. High-throughput mechanical exfoliation of large-scale MoS_2 and WSe_2 was carried out using a roll-to-roll setup. Nitto SPV 224 tape was applied on the surfaces of two polyoxymethylene cylinders with a perimeter ratio of 53:23[25]. A bulk van der Waals material was placed on one cylinder, and the system was rotated under moderate pressure (~20–40 N) at ~1500 rpm for 50 s, resulting in uniformly exfoliated large-area flakes adhered to the tape surface. Monolayer MoS_2 flakes were obtained by mechanically exfoliation of bulk MoS_2 crystals using Nitto SPV 224 tape and subsequently transferring the exfoliated flakes onto Gel-Film (WF 4× 6.0 mil). Candidate monolayer regions were first identified by transmission optical microscopy and then confirmed by differential reflectance spectroscopy.[31–33] Monolayer CVD-MoS_2 flakes were grown by chemical vapor

deposition using a NaCl-assisted ambient-pressure CVD approach, following established procedures reported in the literature.[28,29] After growth, the samples were cleaned using the same protocol applied to mechanically exfoliated flakes.

Transfer process

Transfer of large-area high-throughput flakes was carried out by bringing the tape containing the exfoliated flakes into conformal contact with the target substrate, followed by gentle pressing using a cotton swab to promote adhesion. The sample was then annealed on a hotplate at 110 °C for 5 minutes to facilitate the transfer of films composed of MoS_2 or WSe_2 flakes. To ensure high-density coverage of the flakes, multiple sequential transfer steps were employed. For electronic device fabrication, this transfer process was typically repeated 3-5 times. Mechanically exfoliated (manual) monolayer MoS_2 flakes were transferred onto the pre-patterned electrodes using the deterministic dry-transfer technique.[34]

Electrical characterization

The drain-source current versus bias voltage and FET characteristics were measured using home-built probe station and a Keithley 2450 source-meter unit. Additionally, two programmable benchtop power supplies (TENMA, model 72-2715) were connected in series to characterize the FETs output at varying back-gate voltages from -50V to 50V. Devices subjected to annealing were characterized under avacuum of 1.5×10^5 mbar.[38]

Cleaning process

The fabricated FET devices were immersed in 10ml of N-methyl-2-pyrrolidone (NMP, Sigma-Aldrich) and ultrasonicated at 50 °C for 15 minutes or in repeated cycles of 15

minutes using an ultrasonic cleaner (from RS PRO). Subsequently, the devices were rinsed sequentially with acetone and isopropyl alcohol (IPA), and dried with nitrogen. An identical procedure was employed for ultrasonic cleaning using both dimethyl sulfoxide (DMSO, TechniStrip Micro D350) and acetone solutions.

Supporting Information

Supporting Information includes additional figures, experimental procedures, and supplementary data that support the findings presented in the main text.

Supporting Information File 1: Supporting_Information.pdf

File Name: Supporting_Information.pdf

File Format: PDF

Title: Supplementary Figures and Experimental Details

Acknowledgements

ICMM-CSIC authors acknowledge support from the Severo Ochoa Centres of Excellence program through Grant CEX2024-001445-S, funded by MICIU/AEI/10.13039/501100011033. This work was funded by the Ministry of Science and Innovation (Spain) through the projects PDC2023-145920-I00 and PID2023-151946OB-I00) and the European Research Council through the ERC-2024-PoC StEnSo (grant agreement 101185235) and the ERC-2024-SyG SKIN2DTRONICS (grant agreement 101167218). This work was funded by the China Scholarship Council (Project No.202408360065). Y.S was supported by the Ministry of Science and Innovation (Spain) through the project PRE2021-098348. N.J.A. acknowledges grant JDC2023-052025-I funded by MICIU/AEI/10.13039/501100011033 and by FSE+. Z.S. was supported by ERC-CZ program (project LL2101) from Ministry of Education Youth

and Sports (MEYS) and by the project Advanced Functional Nanorobots (reg. No. CZ.02.1.01/0.0/0.0/15_003/0000444 financed by the EFRR).

References

(1) Mak, K. F.; Shan, J. *Nature Photon* **2016**, *10*, 216–226. doi:10.1038/nphoton.2015.282

(2) Geim, A. K.; Novoselov, K. S. *Nature Mater* **2007**, *6*, 183–191. doi:10.1038/nmat1849

(3) Wang, Q. H.; Kalantar-Zadeh, K.; Kis, A.; Coleman, J. N.; Strano, M. S. *Nature Nanotech* **2012**, *7*, 699–712. doi:10.1038/nnano.2012.193

(4) Jariwala, D.; Sangwan, V. K.; Lauhon, L. J.; Marks, T. J.; Hersam, M. C. *ACS Nano* **2014**, *8*, 1102–1120. doi:10.1021/nn500064s

(5) Karnaushenko, D.; Kang, T.; Bandari, V. K.; Zhu, F.; Schmidt, O. G. *Advanced Materials* **2020**, *32*, 1902994. doi:10.1002/adma.201902994

(6) Forati, E.; Dill, T. J.; Tao, A. R.; Sievenpiper, D. *Nat Commun* **2016**, *7*, 13399. doi:10.1038/ncomms13399

(7) Moon, G. D.; Lim, G.-H.; Song, J. H.; Shin, M.; Yu, T.; Lim, B.; Jeong, U. *Adv Mater* **2013**, *25*, 2707–2712. doi:10.1002/adma.201300794

(8) Zhang, X.-R.; Deng, H.-T.; Zeng, X.; Wang, Y.-L.; Huang, P.; Zhang, X.-S. *J. Phys. D: Appl. Phys.* **2023**, *57*, 013001. doi:10.1088/1361-6463/acfaac

(9) Lewenstein, J. C.; Burgin, T. P.; Ribayrol, A.; Nagahara, L. A.; Tsui, R. K. *Nano Lett.* **2002**, *2*, 443–446. doi:10.1021/nl015690z

(10) Castellanos-Gomez, A.; Buscema, M.; Molenaar, R.; Singh, V.; Janssen, L.; van der Zant, H. S. J.; Steele, G. A. *2D Mater.* **2014**, *1*, 011002. doi:10.1088/2053-1583/1/1/011002

(11) Muñoz, R.; López-Elvira, E.; Munuera, C.; Carrascoso, F.; Xie, Y.; Çakıroğlu, O.; Pucher, T.; Puebla, S.; Castellanos-Gomez, A.; García-Hernández, M. *npj 2D Mater Appl* **2023**, *7*, 1–11. doi:10.1038/s41699-023-00419-8

(12) Zhao, Q.; Wang, W.; Carrascoso-Plana, F.; Jie, W.; Wang, T.; Castellanos-Gomez, A.; Frisenda, R. *Materials Horizons* **2020**, *7*, 252–262. doi:10.1039/C9MH01020C

(13) Puebla, S.; Pucher, T.; Rouco, V.; Sanchez-Santolino, G.; Xie, Y.; Zamora, V.; Cuellar, F. A.; Mompean, F. J.; Leon, C.; Island, J. O.; Garcia-Hernandez, M.; Santamaria, J.; Munuera, C.; Castellanos-Gomez, A. *Nano Lett.* **2022**, *22*, 7457–7466. doi:10.1021/acs.nanolett.2c02395

(14) Xie, Y.; Çakıroğlu, O.; Hu, W.; He, K.; Puebla, S.; Pucher, T.; Zhao, Q.; Ma, X.; Munuera, C.; Castellanos-Gomez, A. *Nano Res.* **2023**, *16*, 5042–5046. doi:10.1007/s12274-022-5241-2

(15) Groenendijk, D. J.; Buscema, M.; Steele, G. A.; Michaelis de Vasconcellos, S.; Bratschitsch, R.; van der Zant, H. S. J.; Castellanos-Gomez, A. *Nano Lett.* **2014**, *14*, 5846–5852. doi:10.1021/nl502741k

(16) Steckenreiter, V.; Hensen, J.; Knorr, A.; Kajari-Schröder, S.; Brendel, R. *IEEE Journal of Photovoltaics* **2016**, *6*, 783–790. doi:10.1109/JPHOTOV.2016.2545406

(17) Ward, J. S.; Remo, T.; Horowitz, K.; Woodhouse, M.; Sopori, B.; VanSant, K.; Basore, P. *Progress in Photovoltaics: Research and Applications* **2016**, *24*, 1284–1292. doi:10.1002/pip.2776

(18) Cheng, C.-W.; Shiu, K.-T.; Li, N.; Han, S.-J.; Shi, L.; Sadana, D. K. *Nat Commun* **2013**, *4*, 1577. doi:10.1038/ncomms2583

(19) Bhalla, V.; Carrara, S.; Stagni, C.; Samorì, B. *Thin Solid Films* **2010**, *518*, 3360–3366. doi:10.1016/j.tsf.2009.10.022

(20) Stan, D.; Mirica, A.-C.; Iosub, R.; Stan, D.; Mincu, N. B.; Gheorghe, M.; Avram, M.; Adiaconita, B.; Craciun, G.; Bocancia Mateescu, A. L. *Processes* **2022**, *10*, 723. doi:10.3390/pr10040723

(21) Fakhr, M. H.; Beshchasna, N.; Balakin, S.; Carrasco, I. L.; Heitbrink, A.; Göhler, F.; Rösch, N.; Opitz, J. *Sci Rep* **2022**, *12*, 20431. doi:10.1038/s41598-022-23395-3

(22) Paupy, N.; Elhmaidi, Z. O.; Chapotot, A.; Hanuš, T.; Arias-Zapata, J.; Ilahi, B.; Heintz, A.; Mbeunmi, A. B. P.; Arvinte, R.; Reza Aziziyan, M.; Daniel, V.; Hamon, G.; Chrétien, J.; Zouaghi, F.; Ayari, A.; Mouchel, L.; Henriques, J.; Demoulin, L.; Mamoudou Diallo, T.; Provost, P.-O.; Pelletier, H.; Volatier, M.; Kurstjens, R.; Cho, J.; Courtois, G.; Dessein, K.; Arcand, S.; Dubuc, C.; Jaouad, A.; Quaegebeur, N.; Gosselin, R.; Machon, D.; Arès, R.; Darnon, M.; Boucherif, A. *Nanoscale Advances* **2023**, *5*, 4696–4702. doi:10.1039/D3NA00053B

(23) Lee, K. P.; Chromey, N. C.; Culik, R.; Barnes, J. R.; Schneider, P. W. *Fundamental and Applied Toxicology* **1987**, *9*, 222–235. doi:10.1016/0272-0590(87)90045-5

(24) Basma, N. S.; Headen, T. F.; Shaffer, M. S. P.; Skipper, N. T.; Howard, C. A. *J. Phys. Chem. B* **2018**, *122*, 8963–8971. doi:10.1021/acs.jpcb.8b08020

(25) Sozen, Y.; Riquelme, J. J.; Xie, Y.; Munuera, C.; Castellanos-Gomez, A. *Small Methods* **2023**, *7*, 2300326. doi:10.1002/smtd.202300326

(26) Sozen, Y.; Pucher, T.; Kesavan, B. P.; Jimenez-Arevalo, N.; Hernandez-Ruiz, J.; Sofer, Z.; Munuera, C.; Riquelme, J. J.; Castellanos-Gomez, A. Wafer-Scale Films of Two-Dimensional Materials via Roll-to-Roll Mechanical Exfoliation. arXiv November 10, 2025. doi:10.48550/arXiv.2511.06960

(27) Eglītis, R.; Kiisk, V.; Kodu, M.; Vanags, M.; Jaaniso, R.; Šmits, K.; Šutka, A. *ACS Appl. Eng. Mater.* **2024**, *2*, 649–658. doi:10.1021/acsaenm.3c00727

(28) Xie, Y.; Wang, Z.; Zhan, Y.; Zhang, P.; Wu, R.; Jiang, T.; Wu, S.; Wang, H.; Zhao, Y.; Nan, T.; Ma, X. *Nanotechnology* **2017**, *28*, 084001. doi:10.1088/1361-6528/aa5439

(29) Yang, H.; Hu, R.; Wu, H.; He, X.; Zhou, Y.; Xue, Y.; He, K.; Hu, W.; Chen, H.; Gong, M.; Zhang, X.; Tan, P.-H.; Hernández, E. R.; Xie, Y. *Nano Lett.* **2024**, *24*, 2789–2797. doi:10.1021/acs.nanolett.3c04815

(30) Pucher, T.; Bastante, P.; Parenti, F.; Xie, Y.; Dimaggio, E.; Fiori, G.; Castellanos-Gomez, A. *npj 2D Mater Appl* **2023**, *7*, 1–6. doi:10.1038/s41699-023-00436-7

(31) Taghavi, N. S.; Gant, P.; Huang, P.; Niehues, I.; Schmidt, R.; Michaelis de Vasconcellos, S.; Bratschitsch, R.; García-Hernández, M.; Frisenda, R.; Castellanos-Gomez, A. *Nano Res.* **2019**, *12*, 1691–1695. doi:10.1007/s12274-019-2424-6

(32) Niu, Y.; Gonzalez-Abad, S.; Frisenda, R.; Marauhn, P.; Drüppel, M.; Gant, P.; Schmidt, R.; Taghavi, N. S.; Barcons, D.; Molina-Mendoza, A. J.; De Vasconcellos, S. M.; Bratschitsch, R.; Perez De Lara, D.; Rohlfing, M.; Castellanos-Gomez, A. *Nanomaterials* **2018**, *8*, 725. doi:10.3390/nano8090725

(33) Frisenda, R.; Niu, Y.; Gant, P.; Molina-Mendoza, A. J.; Schmidt, R.; Bratschitsch, R.; Liu, J.; Fu, L.; Dumcenco, D.; Kis, A.; De Lara, D. P.; Castellanos-Gomez, A. *J. Phys. D: Appl. Phys.* **2017**, *50*, 074002. doi:10.1088/1361-6463/aa5256

(34) Xie, Y.; Castellanos-Gomez, A. **2023**. doi:10.5281/zenodo.7525517

(35) Carrascoso, F.; Pucher, T.; Castellanos-Gomez, A. **2025**. doi:10.5281/zenodo.15148409

(36) Velický, M.; Donnelly, G. E.; Hendren, W. R.; McFarland, S.; Scullion, D.; DeBenedetti, W. J. I.; Correa, G. C.; Han, Y.; Wain, A. J.; Hines, M. A.; Muller, D. A.; Novoselov, K. S.; Abruña, H. D.; Bowman, R. M.; Santos, E. J. G.; Huang, F. *ACS Nano* **2018**, *12*, 10463–10472. doi:10.1021/acsnano.8b06101

(37) Liu, F.; Wu, W.; Bai, Y.; Chae, S. H.; Li, Q.; Wang, J.; Hone, J.; Zhu, X.-Y. *Science* **2020**, *367*, 903–906. doi:10.1126/science.aba1416

(38) Carrascoso, F.; Pucher, T.; Castellanos-Gomez, A. *Zonodo* **2025**, 15148408